12 Controlled Synthesis of Carbon Nanotubes and their Field Emission Properties

Shoushan Fan*, Liang Liu, Zhihao Yuan and Leimei Sheng
Department of Physics and Tsinghua-Foxconn Nanotechnology Laboratory, Tsinghua University, Beijing 100084, China

The synthesis of massive arrays of monodispersed carbon nanotubes that are self-oriented on patterned porous silicon and plain silicon substrates has been developed. The approach involves chemical vapor deposition, catalytic particle size control by substrate design, nanotube positioning by patterning, and nanotube self-assembly for orientation. Based on this technology, a ^{13}C isotope labeling method was developed for revealing the growth mechanism of the multi-walled nanotubes (MWNT) made by chemical vapor deposition (CVD), a topic that has been under extensive investigation since the discovery of the carbon nanotube. Various theoretical models of nanotube growth have been suggested, however, direct experimental evidence to support any of the models is scarce. The isotope labeling method established a relationship between the feeding sequence of $^{13}C_2H_4$ and $^{12}C_2H_4$ and the locations of ^{13}C and ^{12}C atoms in the nanotubes relative to the catalyst particles. The results provided unambiguous evidence supporting the extrusion growth model of MWNTs. Moreover, the isotope labeling method represents a reliable chemical approach to nanotube intra-molecular junctions that may exhibit interesting and useful properties.

The field emission and doping properties of a single multi-walled carbon nanotube has been studied. The threshold voltage was significantly reduced after doping with potassium. The current-voltage measurements fit the Fowler-Nordheim equation. Well-ordered nanotubes can be used as electron field emission arrays. Scaling up of the synthesis process should be entirely compatible with the existing semiconductor processes, and should allow the development of nanotube devices integrated into silicon technology.

SELF-ORIENTED REGULAR ARRAYS OF CARBON NANOTUBES

Well-aligned nanotubes with uniform diameters were synthesized by Fan et al. (1999) on porous silicon as well as plain silicon wafers (Fig. 1). The porous silicon samples were obtained by electrochemical etching of P-doped n^+-type Si(100) wafers in HF solution, and patterned with 5 nm of Fe by electron evaporating through a shadow mask, the substrates were then annealed in air at 300 °C overnight. The synthesis of carbon nanotubes was carried out in a 2-inch quartz tube reactor at 700 °C, ethylene was flown at 1000 sccm for 15 to 60 min.

* Corresponding author. Email: fss-dmp@mail.tsinghua.edu.cn

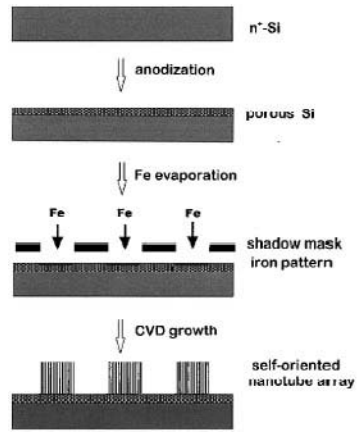

Fig. 1. Schematic process flow for the synthesis of regular arrays of oriented nanotubes on porous silicon by catalyst patterning and CVD.

Three-dimensional regular arrays of nanotube blocks or towers were formed on top of the patterned iron squares on the substrates (Fig. 2). Each nanotube block exhibits very sharp edges and corners, and no nanotubes are observed branching away from the blocks. The width of the blocks is the same as that of the iron patterns. The nanotubes within the blocks are well aligned along the direction perpendicular to the surface (Fig. 2F). TEM investigation showed that 90% of the

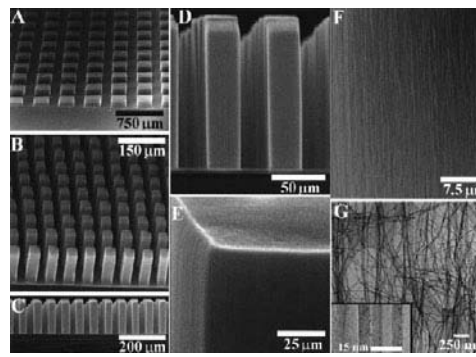

Fig. 2. Electron micrographs of self-oriented nanotubes synthesized on n^+-type porous silicon substrates. (A) SEM image of nanotube blocks synthesized on 250 μm by 250 μm catalyst patterns. (B) Nanotube towers synthesized on 38 μm by 38 μm catalyst patterns. The nanotubes are 130 μm long. (C) Side view of the nanotube towers in (B). The nanotubes self-assemble such that the edges of the towers are perfectly perpendicular to the substrate. (D) Nanotube "twin towers," a zoom-in view of Fig. 2C. (E) Sharp edges and corners at the top of a nanotube tower. (F) SEM image showing that nanotubes in a block are well aligned to the direction perpendicular to the substrate surface. (G) TEM image of pure multi-walled nanotubes in nanotube blocks. The inset is a high-resolution TEM image that shows two nanotubes bundling together. The well-ordered graphitic lattice fringes of both nanotubes are resolved.

multi-walled nanotubes have diameters of 16±2 nm. High-resolution TEM images show low defect density in some sections of nanotube lengths.

Porous silicon substrates exhibit important advantages over plain silicon substrates for synthesizing self-oriented nanotubes, the nanotubes growth at a higher rate (length per minute) on porous silicon than on plain silicon. This can be attributed to ethylene molecules permeating the porous silicon structures and feed the nanotube growth more efficiently. Also, the nanoporous silicon layer acts as an excellent catalyst support. During the 300 °C annealing step, iron oxide nanoparticles form with a narrow size distribution because of their strong interactions with the highly porous support. These strong interactions also prevent catalyst particles from sintering at elevated temperatures.

ISOTOPE LABELING OF CARBON NANOTUBES AND FORMATION OF ^{12}C-^{13}C NANOTUBE JUNCTIONS

The ^{13}C labeling method was applied to the CVD synthesis of carbon nanotubes by Liu and Fan (2001), it involved feeding ^{12}C and ^{13}C isotope ethylene successively in designed sequences to grow aligned MWNT arrays containing intra-tube ^{12}C-^{13}C junctions. The alignment of nanotubes allowed post-growth microscopy and chemical analysis along the nanotubes. Small bundles of MWNTs were pulled out from the array with a tungsten tip and carefully transferred onto a TEM grid, with their top and bottom ends recognized, the Fe catalysts were found only at the bottom end of the nanotubes by TEM and EDX (Fig. 3b-d). The ^{12}C and ^{13}C isotope portions of the nanotubes were clearly identified by a micro-Raman spectroscopy (514 nm laser, 1 μm^2 illumination spot) on the side face of the MWNT array, therefore a relationship was established between the feeding sequence of $^{13}C_2H_4$ and $^{12}C_2H_4$ and the locations of ^{13}C and ^{12}C atoms in the nanotubes relative to the catalyst particles, and hence to provide a direct experimental picture for the CVD growth of carbon nanotubes.

During the 1-minute growth process, ^{12}C ethylene was first introduced for 15 s and then ^{13}C ethylene for another 45 s. Micro-Raman spectra revealed that at the top of the nanotubes arrays, the nanotubes consist of purely ^{12}C, while at the bottom, the nanotubes consist of mostly ^{13}C (Fig. 3f). Since ^{12}C was fed into the system previous to ^{13}C, the result clearly reveals that the top segments of the nanotubes are formed chronically earlier in the growth process than the lower segments. Combined with the finding that the catalyst particles reside at the bottom of the nanotube array, this leads to a clear extrusion growth picture of the nanotubes, as schematically shown in Fig. 4. Inversed isotope feeding sequence leads to the same conclusion.

It should be noted that the top segments of the nanotubes consist of only the first introduced isotope carbon atoms, moreover, TEM observations reveal that the nanotubes are composed of graphitic shells parallel to the tube axis and that the numbers of shells are constant throughout the lengths of the nanotubes. Two conclusions can be drawn from these results. First, all the graphitic shells of the nanotube extrude from the catalyst particle; no direct deposition occurs on the grown tube stem. The absence of such over-coating is desired in terms of synthesizing clean nanotubes for device applications. Second, no separate graphitic shell extrudes over other shells either in the outside or inside of the nanotube.

Therefore, we can come to the conclusion of synchronized extrusion for all the shells of the multi-walled nanotubes from the catalyst.

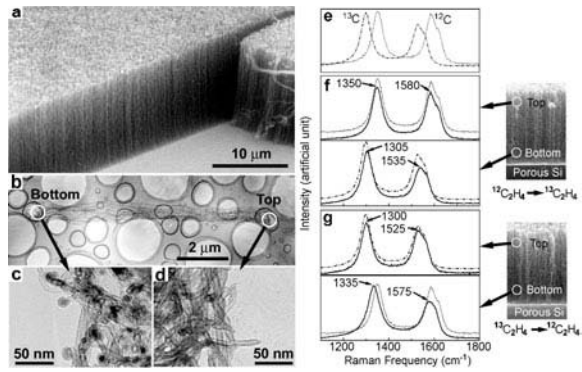

Fig. 3. Isotope-labeled MWNT arrays grown on porous silicon substrates and their micro-Raman spectra. (a) SEM picture of an as-grown MWNT array. (b) TEM image of a bundle of nanotubes, the left end is the bottom, and the right end is the top. (c) A zoomed-in view of the bottom side of (b), darker particles are catalytic iron particles. (d) A zoomed-in view of the topside of (b), capped nanotube tips are visible. (e) Pure ^{12}C nanotube array (dotted) and pure ^{13}C nanotube array (dash dotted) spectra. (f) Nanotube arrays grown with ^{12}C ethylene first and then ^{13}C ethylene. (g) Nanotube arrays grown with ^{13}C ethylene first and then ^{12}C ethylene. The solid curves in the left plots are Raman spectra recorded at the locations circled in the right-hand side images; pure ^{12}C or ^{13}C spectra are also plotted for comparison (up shifted for clarity).

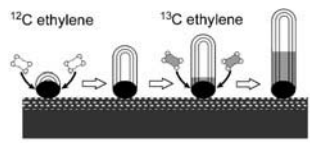

Fig. 4. Growth model of MWNTs. The black oval is the metal catalyst attached to the substrate (white dotted region), the shaded zone in the nanotube and the ethylene molecular represents the ^{13}C isotope atoms. Four snapshots from left to right show the growth process of a ^{12}C-^{13}C nanotube junction.

FIELD EMISSION PROPERTIES OF CARBON NANOTUBES

Carbon nanotubes have been identified as promising candidates for field emitters in applications such as flat panel displays, and these novel devices calls for scaling up nanotube growth and large-scale nanotube assembly and patterning. Fan et al. (1999) found that self-oriented nanotube arrays exhibit low operating voltages and high current stability without further sample processing (Fig. 5). To reach current densities of 1 mA/cm^2 and 10 mA/cm^2, the electric fields (calculated by using the distance from the anode to the top of nanotube blocks) required are 2.7 to 3.3 and 4.8 to 6.1 V/μm, comparable to the best field emission samples previously constructed by processing arc-discharge multi-walled or single-walled nanotubes (the corresponding electric fields are ~3 and ~5 V/mm).

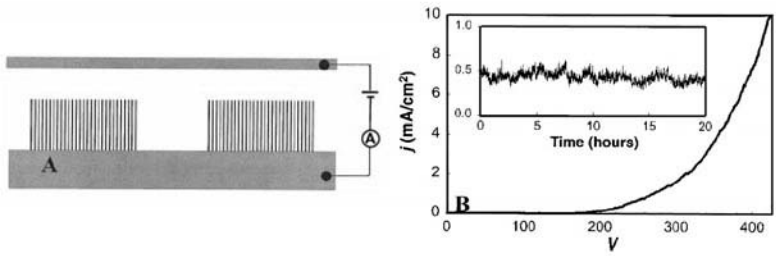

Fig. 5. Self-oriented nanotube arrays as electron field emitter arrays. (A) Experimental setup. The anode and is kept 200 μm away from the sample by a mica spacer. (B) Current density (j) versus voltage (V) characteristics of the sample. The data were taken in a vacuum chamber at 3×10^{-7} torr and were highly reproducible. The inset shows the emission current stability over a test period of 20 hours at a current density of ~0.5 mA/cm^2. The emission current fluctuates but does not exhibit degradation.

Yuan et al. (2001) synthesized highly ordered monodispersed carbon nanotube arrays by CVD growth in a self-ordered hexagonal nanopore anode aluminum oxide (AAO) template. The pore diameter of the template was ~50 nm with the interpore spacing of ~100 nm. The resultant carbon nanotubes are monodispersed and have open ends with uniform sizes (Fig. 6a); such a structure provides high density of emission tips but without field screening effect. The arrays exhibited excellent field emission properties after the underlying oxide layer of the template was removed, the threshold electric field is 2.8 V/μm and the emission current density reaches 0.08 mA/cm^2 at 3.6 V/μm. The I–V characteristic fits the Fowler–Nordheim equation well in the low-field region (Fig 6b).

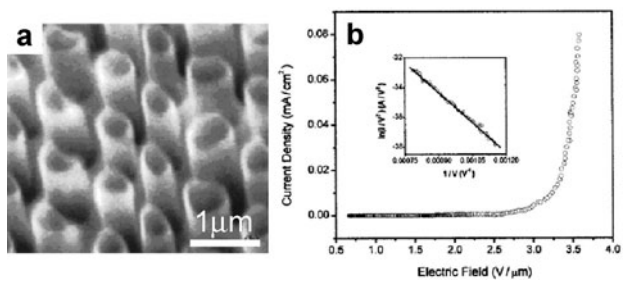

Fig. 6. Highly ordered carbon nanotube arrays grown on the AAO template. (a) After partially etching away the AAO template in NaOH solution. (b) Field emission current density vs. electric field. The anode–sample spacing was 300 μm. Inset: Corresponding Fowler–Nordheim plot.

Hu et al. (2001) investigated the field emission properties of a single multi-walled carbon nanotube tip, they found that the threshold voltage could be significantly reduced by doping the nanotube with potassium (Fig. 7). A single MWNT was mounted on an etched tungsten wire using conductive paste (Fig. 7a), and placed 300 μm apart from the anode. Field emission I-V curve was first measured before the doping (1 in Fig 7b), then potassium was evaporated onto the nanotube tip by an electric heater in the vicinity, the threshold voltage was found to

reduce significantly from 143 V to 76 V immediately after the doping, which is the lowest extraction voltage of a single MWNT tip to the present (2 in Fig. 7b). After continuous field emission at 95 V for 4 min, the emission curve shifted to curve 3 in Fig. 7b, and a final position of curve 4 is reached after strong emission under 163 V and 1.2 μA for 10 min, the curve 4 exhibited no more changes even the MWNT tip was exposed to air. The Fowler-Nordheim theory is applicable up to about 100 nA of emission current before and after doping, and the slopes S are -3.3×10^3 and -8.9×10^2, respectively. Assuming that the work function of curve 2 is that of the potassium, 2.2 eV, and no geometric configuration change occurred after doping, we can estimate from the two slopes that the work function of the original MWNT tip is 5.3 eV, similar to the 5.0 eV for graphite.

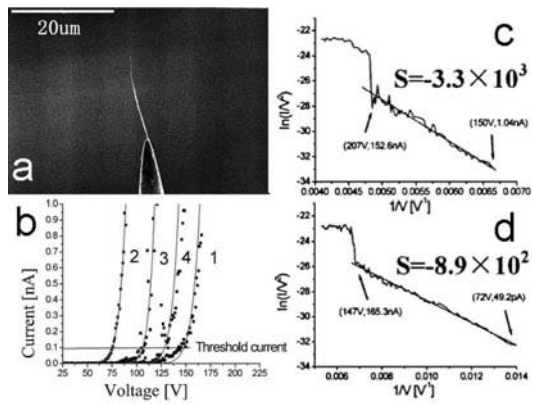

Fig. 7. Field emission of a potassium doped MWNT. (a) Single MWNT mounted on the tip of an etched tungsten wire. (b) Field emission I-V curves at different times. Curve 1, before doping; Curve 2, after doping; Curve 3, after continual field emission at 95 V; Curve 4, after continual field emission at 163 V. (c) Fowler-Nordheim plot of Curve 1. (d) Fowler-Nordheim plot of Curve 2.

REFERENCES

Fan, S. S., Chapline, M. G., Franklin, N. R., Tombler, T. W., Cassell, A. M., and Dai, H. J., 1999, Self-oriented regular arrays of carbon nanotubes and their field emission properties, *Science*, **283**, pp. 512-514.

Hu, B. H., Li, P., Cao, J. E., Dai, H. J., and Fan, S. S., 2001, Field emission properties of a potassium-doped multiwalled carbon nanotube tip, *Japanese Journal of Applied Physics*, **40**, pp. 5121-5122.

Liu, L., and Fan, S. S., 2001, Isotope labelling of carbon nanotubes and formation of ^{12}C-^{13}C nanotube junctions, *Journal of the American Chemical Society*, **123**, pp. 11502-11503.

Yuan, Z. H., Huang, H., Liu, L., and Fan, S. S., 2001, Controlled growth of carbon nanotubes in diameter and shape using template-synthesis method, *Chemical Physics Letters*, **345**, pp. 39-43.

Yuan, Z. H., Huang, H., Dang, H. Y., Cao, J. E., Hu, B. H., and Fan, S. S., 2001, Field emission property of highly ordered monodispersed carbon nanotube arrays, *Applied Physics Letters*, **78**, pp. 3127-3129.